Engineering Science & Technology
http://ojs.wiserpub.com/index.php/EST/

UNIVERSAL WISER PUBLISHER

Research Article

Identification, Uncertain Modelling, and Robust Control of Embedded Systems

Tsonyo Slavov[1], **Jordan Kralev**[1], **Petko Petkov**[1,2*]

[1]Department of Systems and Control, Technical University of Sofia, Sofia, Bulgaria
[2]Bulgarian Academy of Sciences, Bulgaria
E-mail: php@tu-sofia.bg

Received: 6 November 2020; **Revised:** 21 January 2021; **Accepted:** 21 January 2021

Abstract: This paper presents a methodology embodying identification procedures, uncertain modeling, and robust control design of embedded multivariable control systems. Concerning the identification, this methodology involved the determination of probabilistic uncertainty bounds for multivariable plants based on the black box or gray box identification. The bounds obtained were used in the derivation of an uncertain model in the form of upper Linear Fractional Transformation (LFT). This model was used in the robust control design implementing μ-synthesis. The problems arising on the different design stages were illustrated by an example presenting the embedded robust control of a two-input two-output analog model. The plant was identified by using black box and gray box identification methods that produced the necessary information to develop the corresponding uncertainty models. Two discrete-time robust controllers relevant to the two types of identification were designed and embedded in the physical system. Simulation results for the embedded closed-loop system and experimental results obtained by using the robust controllers were compared.

***Keywords*:** embedded control systems, multivariable system identification, uncertainty modeling, robust control

1. Introduction

Recently, there was an increasing interest in the design and implementation of embedded systems, which utilize robust control laws (see [1]-[3]). The modern microcontrollers and Digital Signal Processors (DSP) allow the embedding of sophisticated controllers that realize high order robust control laws. The implementation of such laws provides possibilities to achieve robust stability and performance of the closed-loop systems and to ensure low sensitivity to parameter variations and unknown noises and disturbances.

The design and implementation of robust control laws in embedded systems are associated with several challenges, which can make the design process a nontrivial task. The main difficulty is related to the determination of a plant uncertainty model that is appropriate for the design of a controller satisfying stability and performance requirements to the closed-loop system behavior.

Finding such a model usually requires the application of an identification procedure and a sequence of algorithms for model reduction and uncertainty description. This is followed by the design of a robust controller that may require doing several iterations to determine the desired performance weighting functions. Finally, the controller should be

DOI: https://doi.org/10.37256/est.222021711

implemented in the appropriate hardware and software environment.

2. Plant identification

In practice, it is frequently required to use experimentally obtained input and output data to determine an appropriate plant model. As it is well known [4], a model can be identified by two different approaches named *black box* and *gray box* respectively. The black box approach requires only measurements of system inputs and outputs and does not require information about the plant structure. In this way, the black box models do not explicitly reveal the physical structure and parameters of the plant, but the structure should be sufficiently simple and appropriate for controller design. Aside from input/output measurements, the gray box approach requires information about model structure and in this case, only the plant parameters are estimated. This approach is useful when we can derive model structure from physical principles, but do not know the values of the parameters, including mass, the moment of inertia, friction coefficients, and others. The main advantage of the gray box model is that its variables and parameters have physical interpretation and explicitly reveal the physical relations between these variables. Methods for black box and gray box identification were implemented in various functions of System Identification Toolbox™ [5].

The identification process of linear models involves several issues including:

Experiment design and input/output data acquisition;

Model structure selection;

Estimation of model parameters;

Validation of the estimated model to decide whether the model is adequate for the controller design.

A thorough discussion of these issues can be found in [4], [6]-[8].

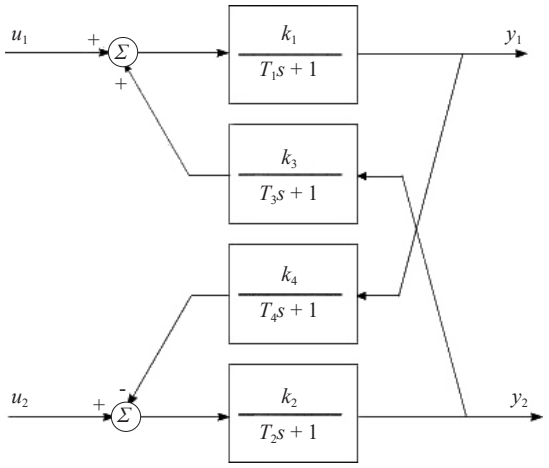

Figure 1. Block-diagram of the analog model

In this paper, as an illustrative example, we considered using the design of an embedded controller for a two-input/two-output control pant with block-diagram, as shown in Figure 1. Due to the cross-coupling between the inputs, the plant is difficult to control by single-input controllers and good performance requires the implementation of a multivariable controller. Physically, the plant is developed by the analog modeling system *Serie 9500 Modulsystem Regelungstechnik* [9] in the form of a board on which blocks with different dynamic functions were arranged (Figure 2).

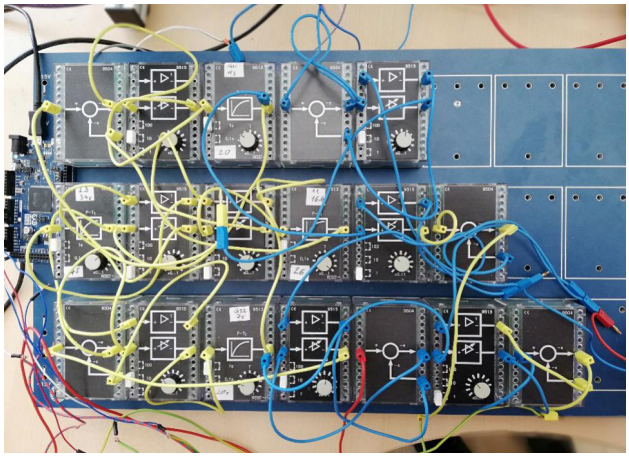

Figure 2. The laboratory set up

The board was powered by a DC supply of ±15 V with the linear range of input and output signals of ±10 V. The gains and time constants were set arbitrarily within the admissible ranges.

Plant identification was done in an open-loop setting. The two models were estimated by the black box and gray box approaches, respectively. To ensure a permanent excitation of the plant, two mutually uncorrelated stochastic binary sequences were used as the input signals to the plant. These signals are of levels 0.5 V and 1.5 V for the first input and 1.5 V and 2.5 V for the second input. The data measured with a sampling period of $T_0 = 0.05$ s were centered and separated into two sets which were used to estimate and validate the model. The set of centered data intended for model estimation is as shown in Figure 3. The sampling period was chosen to be sufficiently smaller than the expected values of the plant time constants.

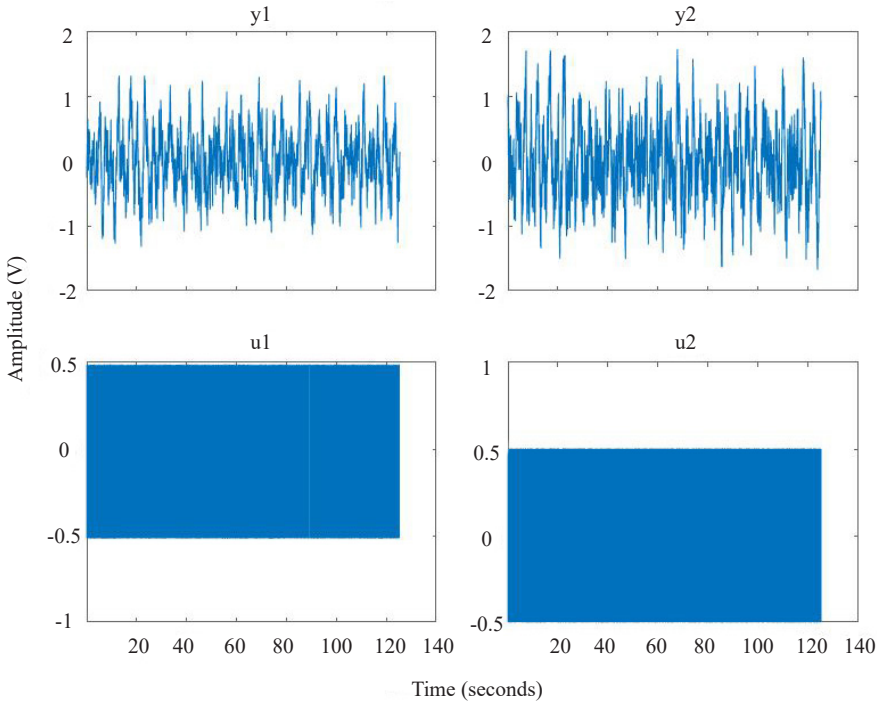

Figure 3. Input/output plant data

To estimate the plant model, the prediction error method for the state-space models [4] was implemented using the function ssest of MATLAB® System Identification Toolbox™ [5]. As a result of the black box identification, a fourth-order model is obtained in the form of

$$x(k+1) = Ax(k) + Bu(k) + Ke(k)$$
$$y(k) = Cx(k) + e(k) \tag{1}$$

where

$x(k) = [x_1(k)\ x_2(k)\ x_3(k)\ x_4(k)]^T$ is the state vector, $u(k) = [u_1(k)\ u_2(k)]^T$ is the input vector, $y(k) = [y_1(k)\ y_2(k)]^T$ is the output vector, and $e(k) = [e_1(k)\ e_2(k)]^T$ is the residue error vector.

The matrices of the obtained model (1) are

$$A = \begin{bmatrix} 0.8827 & -0.07915 & 0.01222 & -0.07701 \\ 0.06725 & 0.8975 & 0.09257 & 0.004242 \\ 0.1435 & 0.06957 & 0.8687 & 0.05017 \\ -0.07528 & 0.1467 & -0.06885 & 0.8521 \end{bmatrix}, \quad B = \begin{bmatrix} 0.00253 & -0.01819 \\ -0.01635 & -0.003845 \\ 0.01057 & 0.01243 \\ 0.01519 & -0.01057 \end{bmatrix},$$

$$K = \begin{bmatrix} 0.002814 & -0.01884 \\ -0.01711 & -0.004601 \\ 0.01819 & 0.004967 \\ 0.009457 & -0.00412 \end{bmatrix}, \quad C = \begin{bmatrix} 5.4 & -23.17 & 1.53 & 1.059 \\ -29.55 & 5.202 & 0.7781 & -1.232 \end{bmatrix}, \quad D = \begin{bmatrix} 0 & 0 \\ 0 & 0 \end{bmatrix}$$

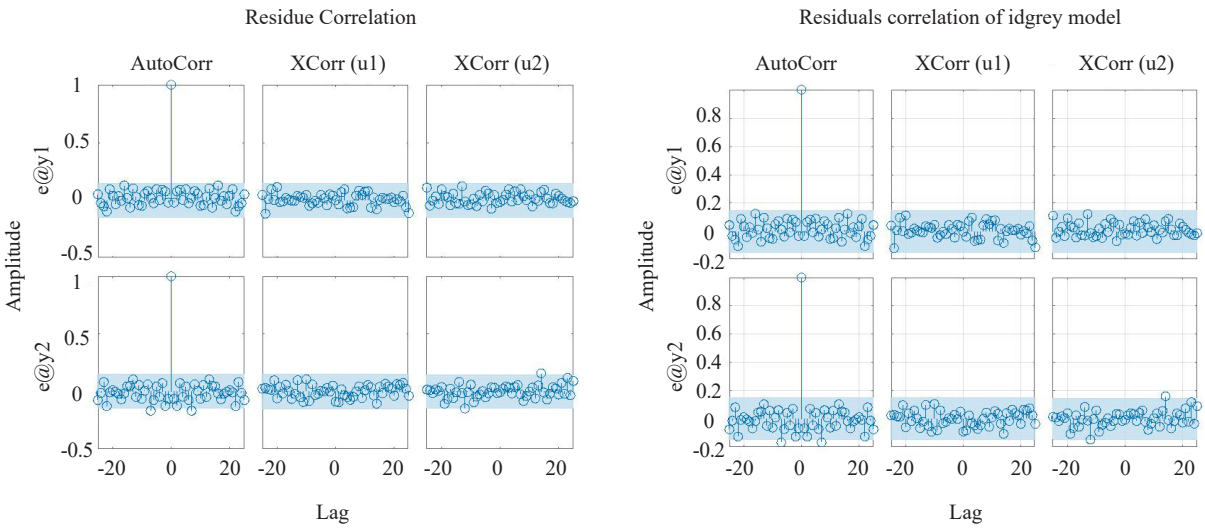

Figure 4. Correlation test for residue error of black-box (left) and gray-box identification models (right)

Model (1) was validated by various tests. The residue correlation tests in the time domain and frequency domain are as shown on the left side of Figure 4 and 5.

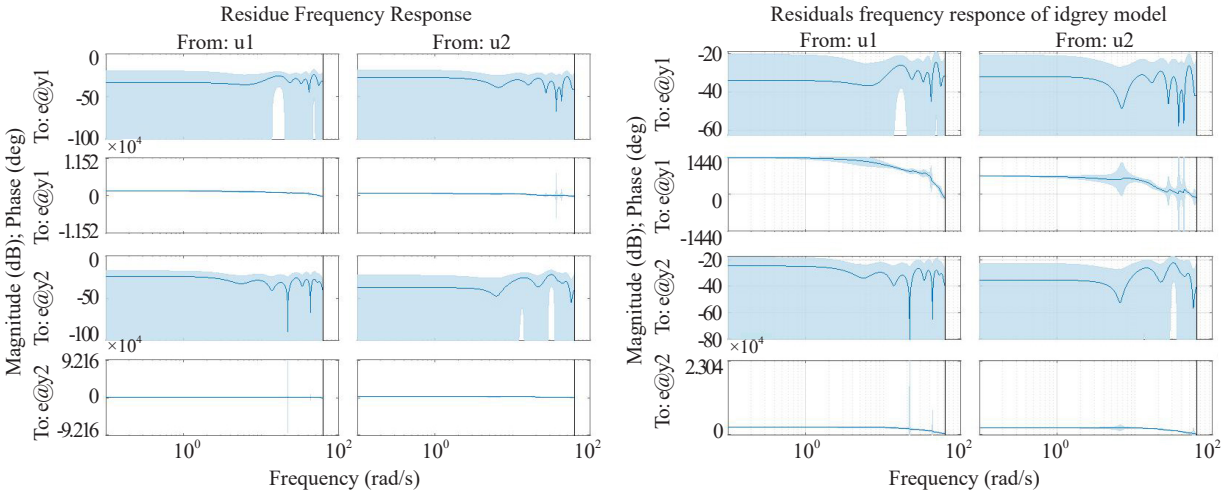

Figure 5. Residue frequency response for the black-box (left) and gray-box (right) identification models

Using the grey box identification procedure a similar fourth-order model is obtained with matrices

$$A=\begin{vmatrix} -\frac{1}{T_1} & 0 & \frac{k_1}{T_1} & 0 \\ 0 & -\frac{1}{T_2} & 0 & \frac{k_2}{T_2} \\ 0 & \frac{k_3}{T_3} & -\frac{1}{T_3} & 0 \\ \frac{k_4}{T_4} & 0 & 0 & -\frac{1}{T_4} \end{vmatrix},\ B=\begin{vmatrix} \frac{k_1}{T_1} & 0 \\ 0 & \frac{k_2}{T_2} \\ 0 & 0 \\ 0 & 0 \end{vmatrix},\ C=\begin{vmatrix} 1 & 0 & 0 & 0 \\ 0 & 1 & 0 & 0 \end{vmatrix},\ D=\begin{vmatrix} 0 & 0 \\ 0 & 0 \end{vmatrix},\ K=\begin{vmatrix} 10.11 & -0.03537 \\ 0.4523 & 12.8 \\ -0.5888 & 0.7359 \\ 0.7508 & -0.7557 \end{vmatrix},$$

$$k_1=2.387,\ k_2=3.135,\ k_3=0.5245,\ k_4=0.421,\ T_1=0.255,\ T_2=0.244,\ T_3=0.888,\ T_4=0.599,$$

The residue correlation tests in the time domain and frequency domain for this model are as shown on the right-hand side of Figure 4 and 5. It is seen from the residue error test for both models that the estimates obtained are unbiased.

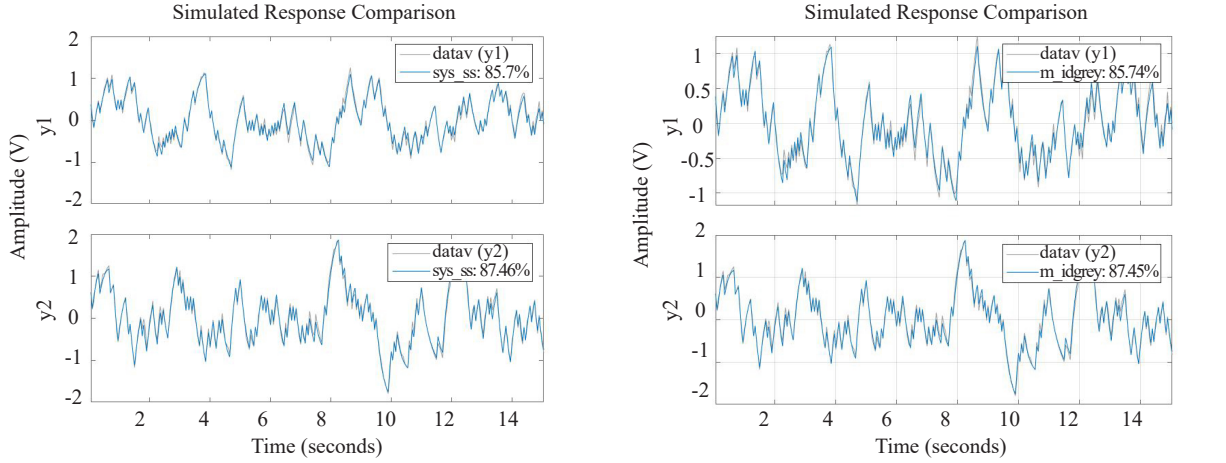

Figure 6. Simulated response comparison for the black-box (left) and gray-box (right) identification models

A comparison of the simulated responses of the two estimated models is as shown in Figure 6. The coincidence of more than 85% between the output signals demonstrated that the model sufficiently describes the plant dynamics well.

3. Derivation of the uncertainty model

The next step after the identification is the determination of the plant uncertainty model. If an analytical description of the plant is not available (this is the most frequent case in practice), it is necessary to derive the uncertainty model based on plant identification results. Using identification to determine uncertain models for robust control has been discussed in several papers (see [10]-[15]). However, practical methods for finding uncertain models through identification using the MATLAB® environment are not widely available.

The derivation of an uncertainty model of a plant using the results from the black box or grey gray box identification of the system was considered. The condition of unbiased parameter estimates obtained by the identification guarantees that the exact parameter values are contained in the confidence intervals of parameter estimates with probability close to 1. This allows us to derive a parametric uncertainty model with scalar uncertainties. However, since the number of estimated parameters is usually large, the implementation of a structured uncertainty model is not practical and it is preferable to derive an unstructured uncertainty model. Based on parameter 3σ confidence intervals, maximum relative deviations from the nominal model in the frequency domain can be obtained. These deviations were parameterized and used to obtain input or output, multiplicative uncertainty model.

The uncertain model in the case of black-box identification was determined in the following way. Based on the estimated model (1) it is possible to estimate the residuals after identification $e(k)$. The estimate of the covariation $e(k)$ is determined from

$$M\left\{e^T e\right\} = \begin{bmatrix} \sigma^2_{e1} & 0 \\ 0 & \sigma^2_{e2} \end{bmatrix}, \tag{2}$$

where the covariation of ith residual $\sigma^2_{e_i}$, $i = 1, 2$ is determined from

$$\sigma^2_{e_i} = \frac{1}{N-1}\sum_{k=1}^{N} e_i^2(k). \tag{3}$$

For unbiased estimates, the estimated parameters have covariations

$$P_{\hat{\theta}} = \sigma^2_{e_i}\left[\frac{1}{N}\sum_{k=1}^{N}\psi(k,\hat{\theta})\psi^T(k,\hat{\theta})\right]^{-1}, \tag{4}$$

where $\hat{\theta}_{40\times1}$ is a vector of estimated parameters (the elements of the matrices A, B, C, K) and $\psi(k,\hat{\theta})_{40\times2}$ is a matrix, whose columns are the gradients of the predicted error in respect to the parameters θ for $\theta = \hat{\theta}$, i.e.,

$$\psi(k,\hat{\theta})_{40\times i} = grad_\theta(y_i(k) - \hat{y}_i(k,\hat{\theta})),\ i = 1,2. \tag{5}$$

The predicted output $\hat{y}(k,\hat{\theta})$ is obtained by the system

$$\begin{aligned} \hat{x}(k+1,\hat{\theta}) &= A\hat{x}(k,\hat{\theta}) + Bu(k) + K(y(k) - C\hat{x}(k,\hat{\theta})) \\ \hat{y}(k,\hat{\theta}) &= C(\theta)\hat{x}(k,\hat{\theta}) \end{aligned} \tag{6}$$

In this way, the standard deviations of the parameter estimates are determined from

$$\sigma_{\theta_u} = \sqrt{P_\theta(i,i)},\ i = 1,2,...40. \tag{7}$$

The model (1) is easily transformed into the transfer matrix

$$W(z,\theta) = \left[C[zI - A]^{-1} B \quad C[zI - A]^{-1} K \right] \tag{8}$$

Based on the standard deviations (7) and Gauss approximation formula [4], it is possible to compute the standard deviations $\Delta W_{ij}(e^{j\omega},\theta)$, $i = 1, 2$, $j = 1, 2$ of the individual elements of the transfer function matrix (8)

$$\Delta W_{ij}(e^{j\omega},\theta) = \sqrt{\frac{1}{N} W'(e^{j\omega},\theta)^T P_\theta W'(e^{j\omega},\theta)},\ i = 1,2,\ j = 1,2 \tag{9}$$

where the matrix $W'(e^{j\omega},\theta)$ is the matrix of the gradients of the elements (8) concerning the estimated parameters θ. Under the condition that the estimates obtained are unbiased, it follows that with the probability of 0.997 one has

$$W_o(e^{j\omega}) \in \left[W(e^{j\omega},\theta) \pm 3\Delta W(e^{j\omega},\theta) \right] \tag{10}$$

where $W_o(e^{j\omega})$ is the "true" transfer function and

$$W(e^{j\omega},\theta) = \begin{bmatrix} W_{11}(e^{j\omega},\theta) & W_{12}(e^{j\omega},\theta) \\ W_{21}(e^{j\omega},\theta) & W_{22}(e^{j\omega},\theta) \end{bmatrix},\ \Delta W(z,\theta) = \begin{bmatrix} \Delta W_{11}(e^{j\omega},\theta) & \Delta W_{12}(e^{j\omega},\theta) \\ \Delta W_{21}(e^{j\omega},\theta) & \Delta W_{22}(e^{j\omega},\theta) \end{bmatrix}.$$

The standard deviations $\Delta W_{ij}(e^{j\omega},\theta)$ are obtained in the form of nonparametric models in the frequency domain (frequency responses). These models should be parametrized to obtain an uncertainty model, which contains the "true" plant description with probability tending to 1. In the given case, it is proposed to use uncertain models with input multiplicative uncertainty such that each transfer function is approximated by

$$G_{ij}(z) = G_{ijnom}(z)(1 + \hat{W}_{ij}(z)\Delta_{ij}),\ i = 1,2,\ \ j = 1,2 \tag{11}$$

where $G_{ijnom}(z) = W_{ij}(z)|\Delta_{ij}| < 1$ are dynamic uncertainties and $\hat{W}_{ij}(z)$ are weighting filters. The filters $\hat{W}_{ij}(z)$ are obtained after approximation (parametrization) of the nonparametric frequency models

$$\frac{3\Delta W_{ij}(e^{j\omega})}{G_{ijnom}(e^{j\omega})},\ i = 1,2,\ j = 1,2, \tag{12}$$

by stable no minimum phase transfer functions of an appropriate order. Note that the division in (12) was done element-wise on each one of the values of the nonparametric model. The approximation itself was done by the function fitmagfrd of MATLAB. As the order of these transfer functions increased, the approximation error decreased while the model order increased. In this case, we use transfer functions W_{11}, W_{12}, W_{21} and W_{22} of the order 9, 3, 3, and 8, respectively, which ensure good coincidence between the approximated and actual magnitude plots. Each element of the multivariable plant (11) may be represented as an input multiplicative uncertainty as shown in Figure 7.

It should be noted that instead of the input multiplicative model (11) it is also possible to use output multiplicative or additive models [17]. The advantage of the multiplicative models is that in this case, one uses relative instead of absolute values of the uncertainty.

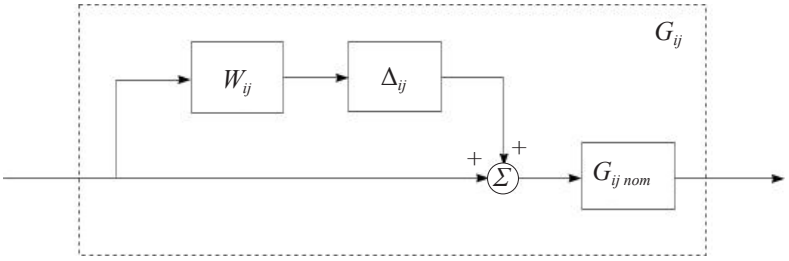

Figure 7. Input multiplicative model of the uncertain element

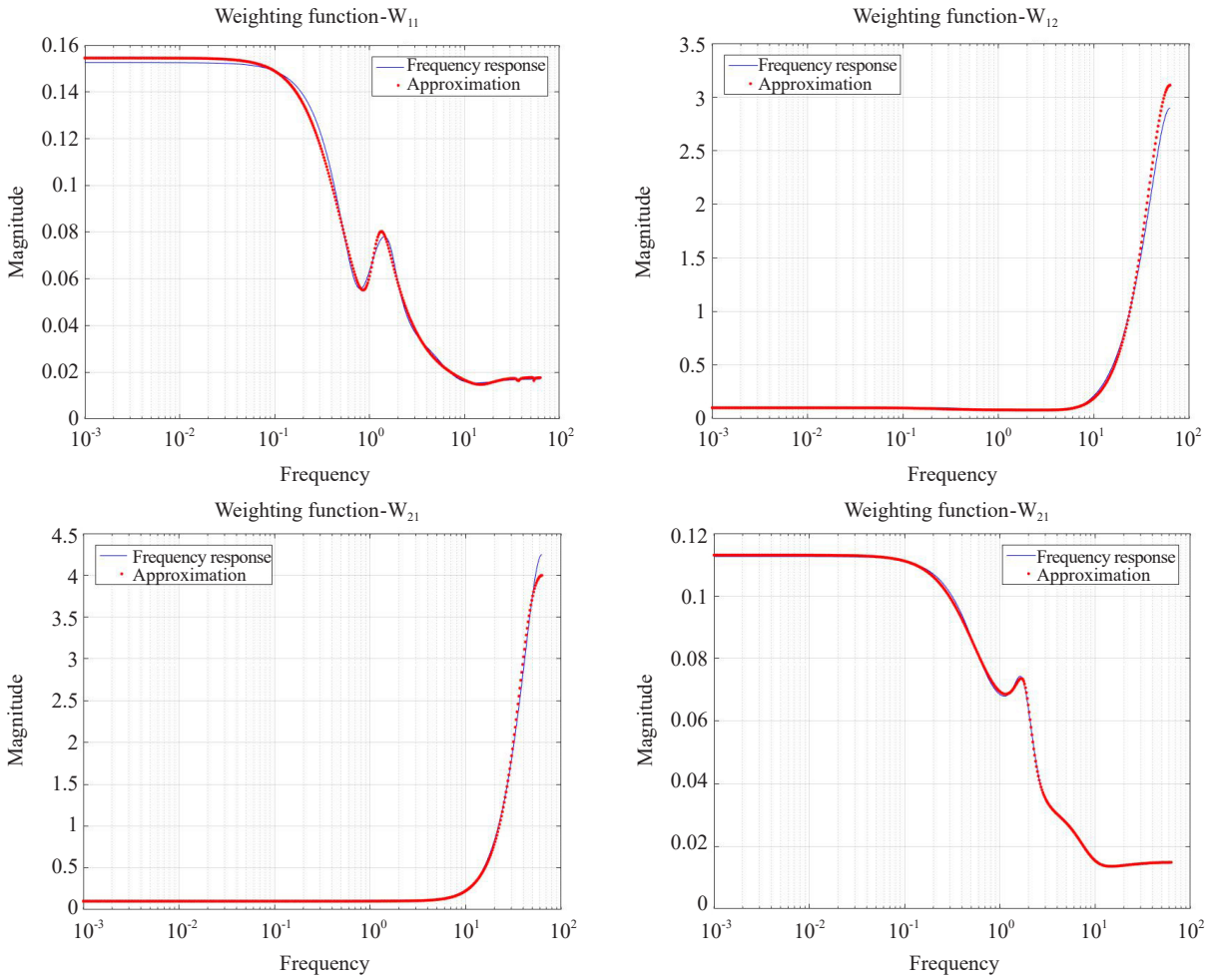

Figure 8. Approximations of the weighted functions obtained for the black-box identification model

The magnitude plots of the weighting functions for the black box identification model are as shown in Figure 8. The approximation of the weighting functions in the case of gray box identification was similarly done. In this case, it is possible to achieve good accuracy using transfer functions of order 3.

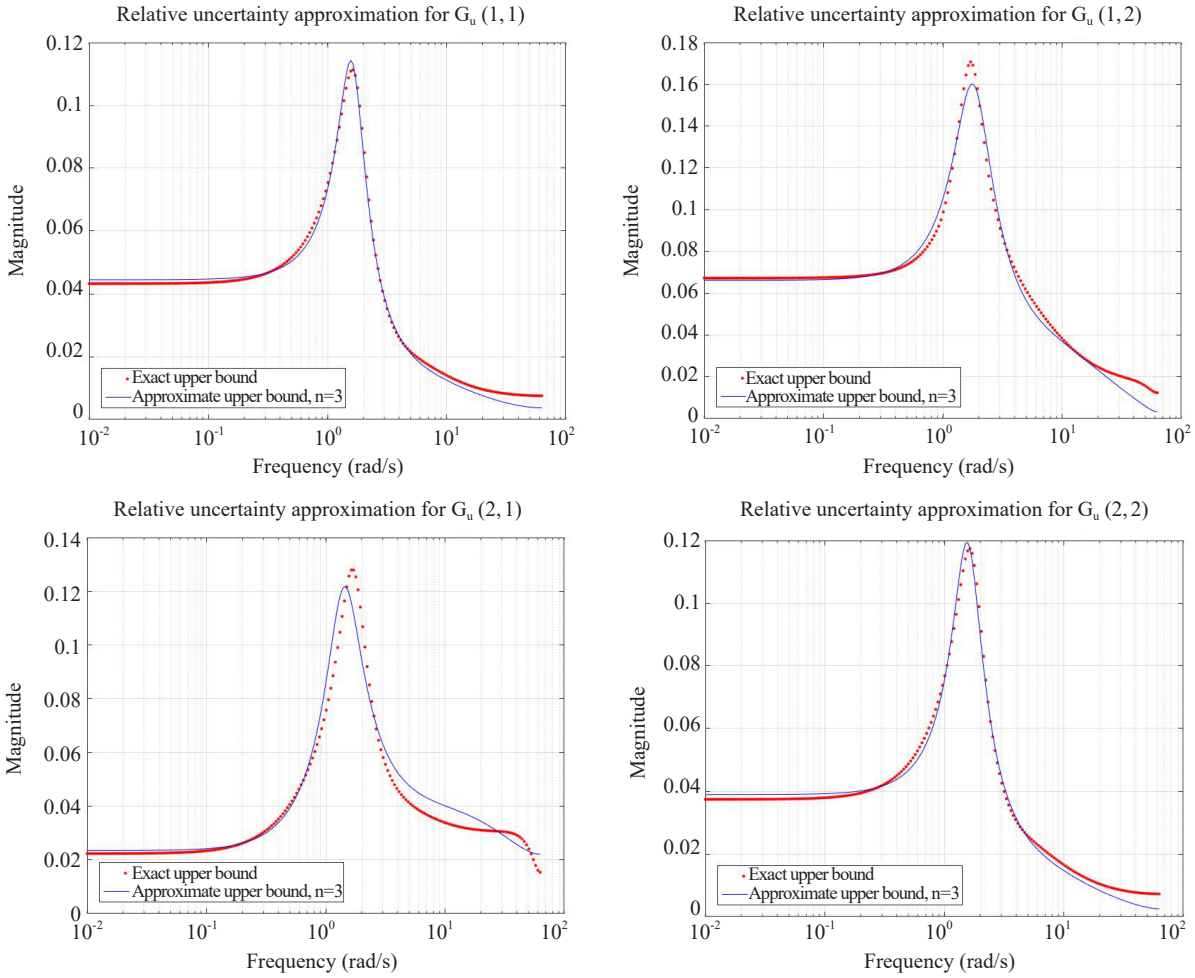

Figure 9. Approximations of the weighted functions obtained for the gray-box identification model

The magnitude plots of the weighting functions for the gray box model are as shown in Figure 9. Clearly, the frequency responses of the relative uncertainties are quite different for both models.

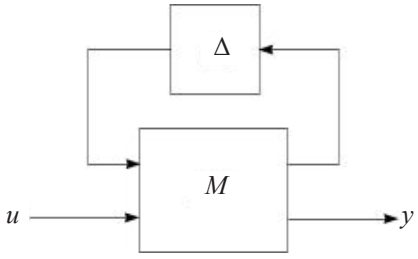

Figure 10. Upper LFT of the uncertain element

For both types of identification, the model (11) is represented in the form of upper LFT as shown in Figure 10. The transfer function M is obtained from the transfer functions $\hat{W}_{ij}(z)$ and $G_{ijnom}(z)$. Δ is a diagonal matrix, containing the uncertainties Δ_{ij}. Due to the presence of the weighting transfer functions, the nominal model M is obtained of a high order-in the case of the black box identification M is of order 156 and in the case of gray box identification, it is of order 112.

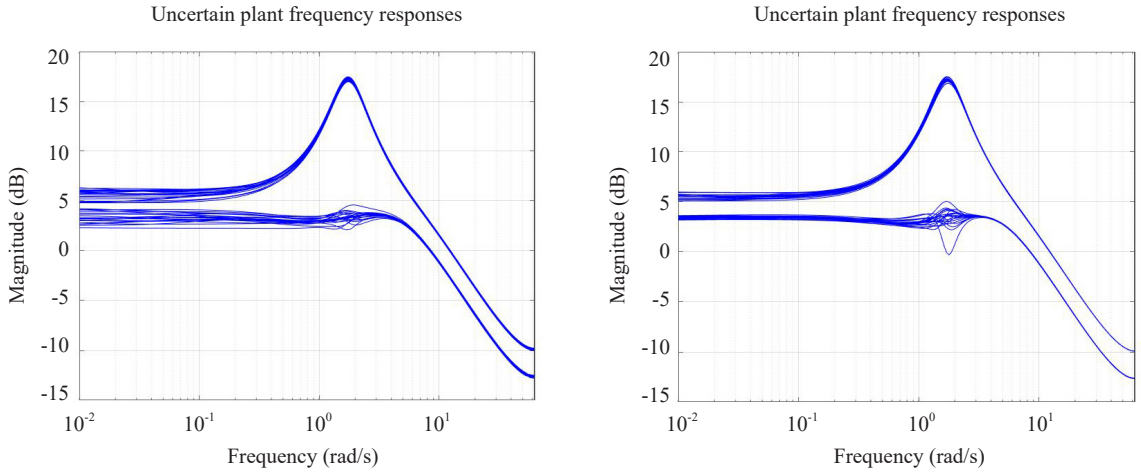

Figure 11. Magnitude plots of the uncertain plants obtained by the black-box identification (left) and the gray-box identification (right)

The magnitude plots of the corresponding uncertain models that possessed close shapes are as shown in Figure 11.

4. Plant model reduction

The high order of the uncertain plant model caused the subsequent controller designing difficult or even impossible. Therefore, the model order is reduced based on the Hankel singular values [16], [17] of the plant.

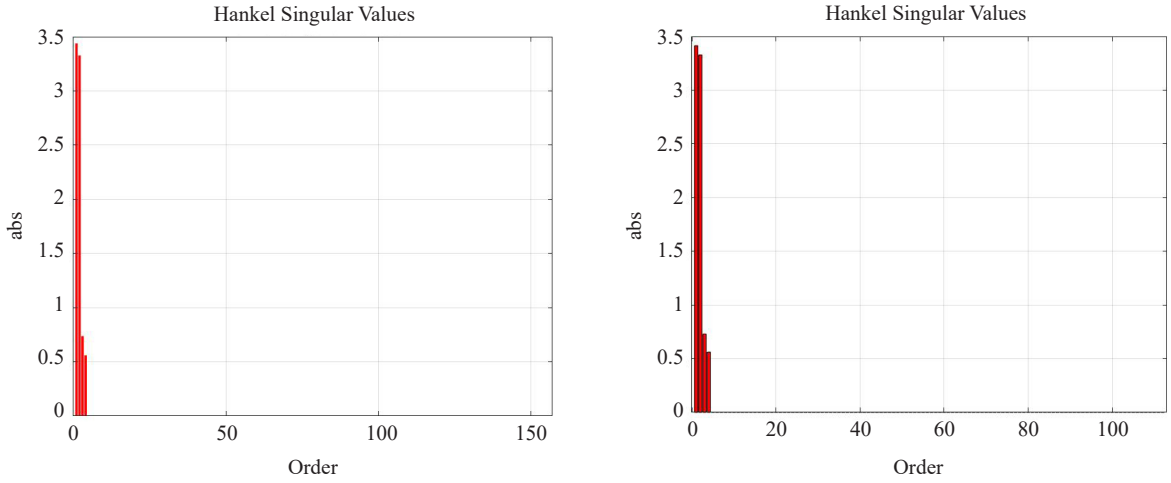

Figure 12. Hankel singular values of the uncertain black-box (left) and the gray-box (right) identification plant models

The Hankel singular values of the uncertain models obtained by the function hankelsv are as shown in Figure 12. It can be seen that only the first four singular values are sufficiently greater than zero so that the next values can be neglected. Hence, both uncertain models can be chosen to be of the order 4. The reduced-order models were obtained by the function reduce from Robust Control Toolbox™.

The magnitude plots of the elements G_{11}, G_{12}, G_{21}, G_{22} and the reduced-order black box model were determined for 20 random values of the uncertain elements along with their corresponding upper and lower bounds (shown by continuous lines) determined for the original model and reduced order model, as shown in Figure 13. It can be seen that the frequency response bounds approximately well with the uncertainties in the corresponding elements.

In the case of gray box identification, the obtained probabilistic bounds on the gains k_1, k_2, k_3, k_4 and time constants T_1, T_2, T_3, T_4. This allows for obtaining a discrete-time uncertainty model with structured uncertainty. Unfortunately, pure structured uncertainty creates numerical difficulties in μ-synthesis, which prevents the usage of such a model. Hence, the uncertainty model was again used with the unstructured uncertainty obtained in the following way. The model parameters were gridded for 100 values of each parameter and the maximum uncertainty of each element G_{ij} is approximated by input multiplicative uncertainty as described above for the case of black-box identification. The frequency responses gridded for 20 values are as shown in Figure 14. Clearly, the derived upper bounds capture well the uncertainties in the corresponding transfer function matrix elements.

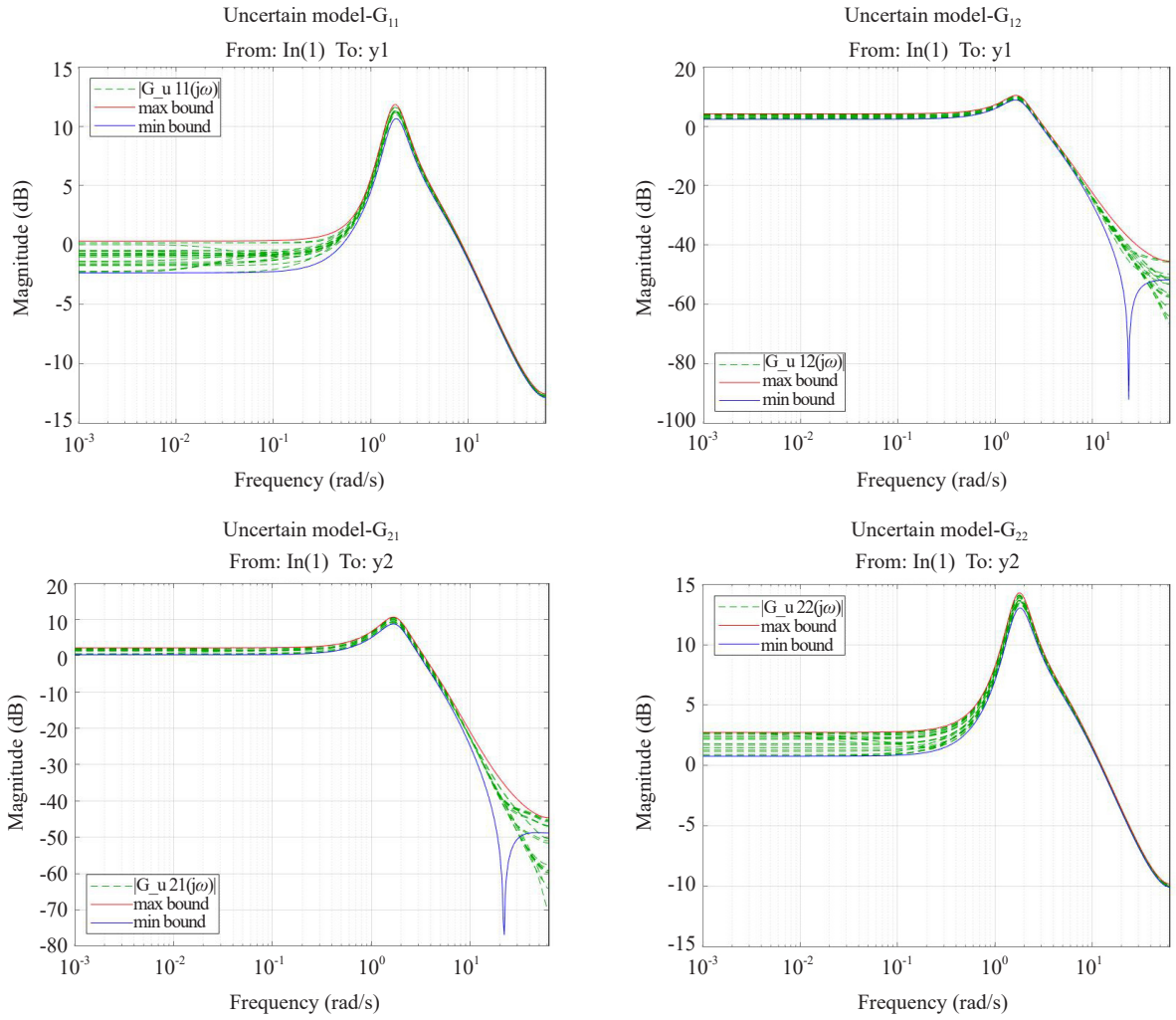

Figure 13. Uncertain frequency responses of the reduced-order model obtained by black-box identification

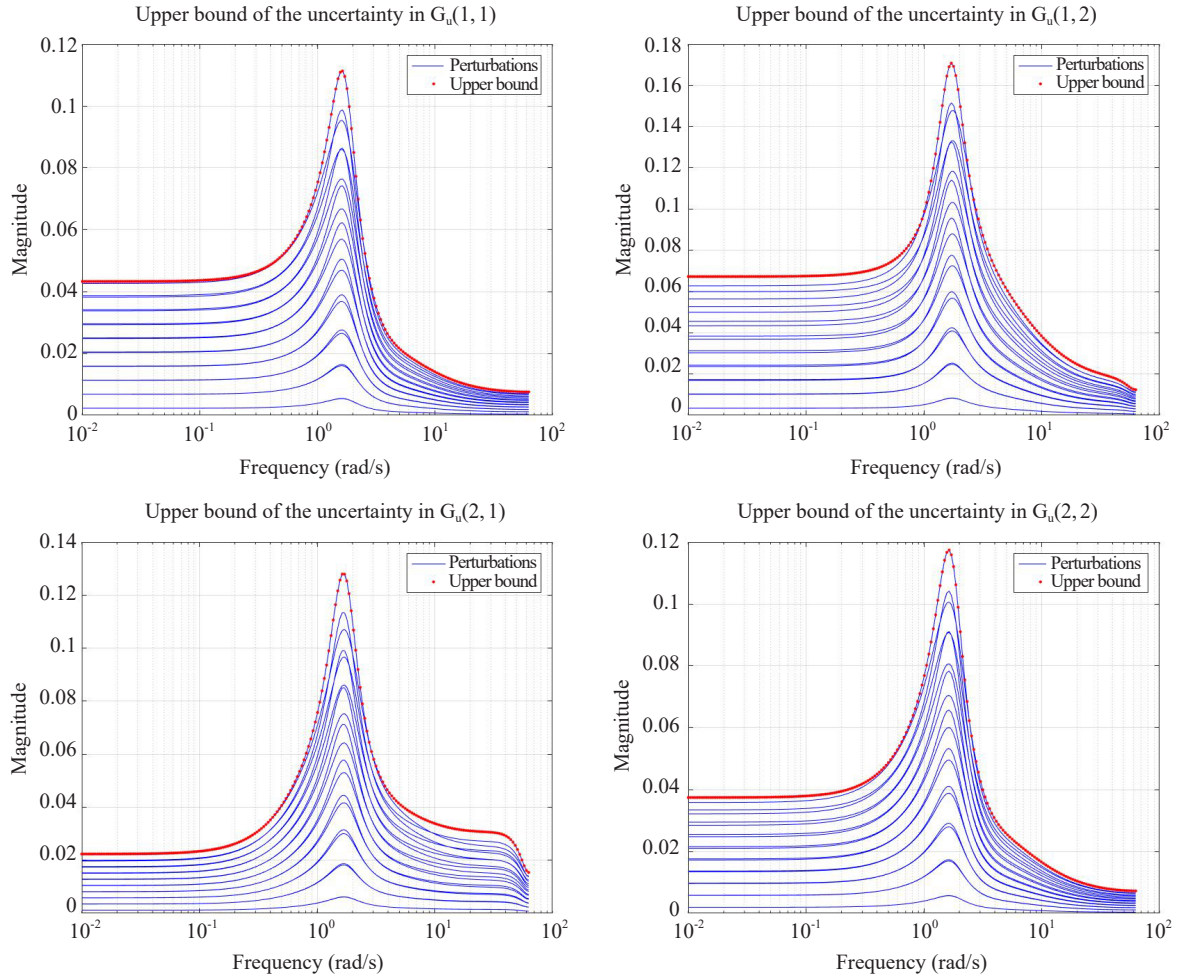

Figure 14. Uncertainties frequency responses for the reduced-order model obtained by gray-box identification

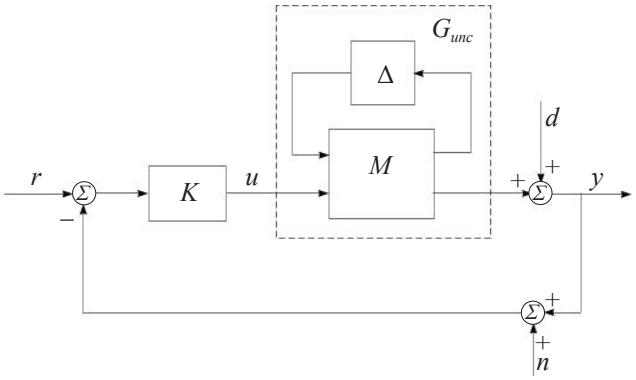

Figure 15. Block-diagram of the uncertain closed-loop system

The block diagram of the closed-loop system relevant to the determined uncertain plant model for both identification methods is as shown in Figure 15, where *d* denotes the plant output disturbances and *n* is the sensor and Analog to Digital Converter (ADC) noises.

5. Robust controller design

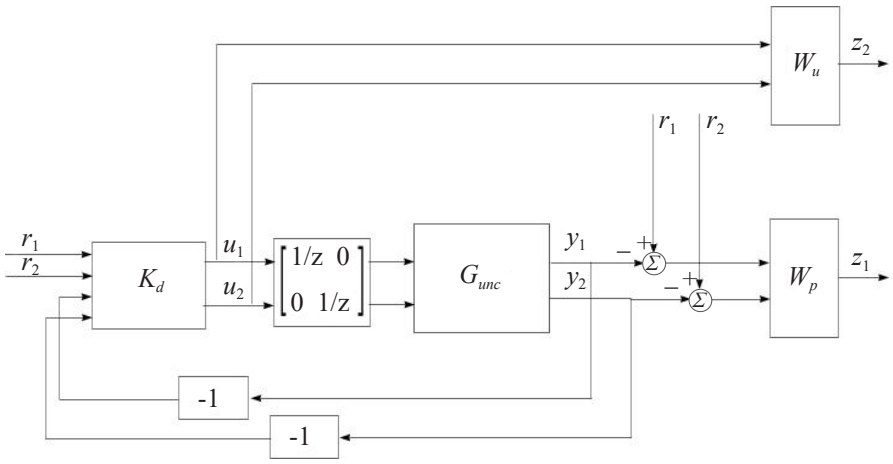

Figure 16. Block-diagram of the closed-loop system

The block diagram of the closed-loop system used in the design of robust controllers which includes the performance W_p and control weighting W_u functions is as shown in Figure 16, which is typical for robust control design [16]-[18]. The transfer function matrix of the uncertain plant is denoted by G_{unc} and the discrete controller to be determined-by K_d. The system has a reference vector $r = [r_1\ r_2]^T$ and an output error vector $z = [z_1\ z_2]^T$. A two degrees-of-freedom controller [17] is used to achieve better performance.

The control action is determined from

$$u = [K_r\ K_y]\begin{bmatrix} r \\ y \end{bmatrix} = K_r r + K_y y \tag{13}$$

where K_r is the prefilter transfer function matrix and K_y is the output controller transfer function.

Thus, the closed-loop system in Figure 16 is described by the equation

$$\begin{bmatrix} z_1 \\ z_2 \end{bmatrix} = \begin{bmatrix} W_p S_o G_{unc} K_r \\ W_u S_i K_r \end{bmatrix} r \tag{14}$$

where $S_o = (I - G_{unc}K_y)^{-1}$ is the output sensitivity transfer function matrix, and $S_i = (I - K_y G_{unc})^{-1}$ is the input sensitivity transfer function matrix. The problem for μ-synthesis is solved by seeking a controller in (13) to satisfy the following conditions [16]-[18].

Robust stability: The closed-loop system is robustly stable if it is internally stable for all admissible uncertainties.

Robust performance: The closed-loop system must be robustly stable and for each admissible, G_{unc}, it is necessary to satisfy the performance requirement

$$\left\| \begin{matrix} W_p S_o G_{unc} K_r \\ W_u S_i K_r \end{matrix} \right\|_\infty < 1 . \tag{15}$$

The performance weighting function W_p is chosen as a low pass filter and the control weighting function W_u as a high pass filter. The design is done for a variety of weighting functions ensuring a good balance between robustness and performance. The final weighting functions for the black box identification model are

$$W_p(p) = diag\left[\frac{1.4(2.5s+1)}{4s+0.1}, \frac{1.2(2s+1)}{4s+0.1}\right],\ W_u(p) = diag\left[\frac{0.04(0.01s+1)}{0.0001s+1}, \frac{0.02(0.01s+1)}{0.0001s+1}\right]$$

and the performance weighting function for the gray box identification model is

$$W_p(p) = diag\left[\frac{1.4(2s+1)}{3s+0.1}, \frac{1.2(2s+1)}{3s+0.1}\right],$$

the control weighting function W_u is the same as in the case of the black box identification model.

For the aim of controller design, the weighting functions are sampled with the sampling interval of 0.05 s. The μ-synthesis is done by the Robust Control Toolbox™ function dksyn [19]. For both models, the controller designed is of 16th order and the corresponding closed-loop system achieves robust stability and robust performance.

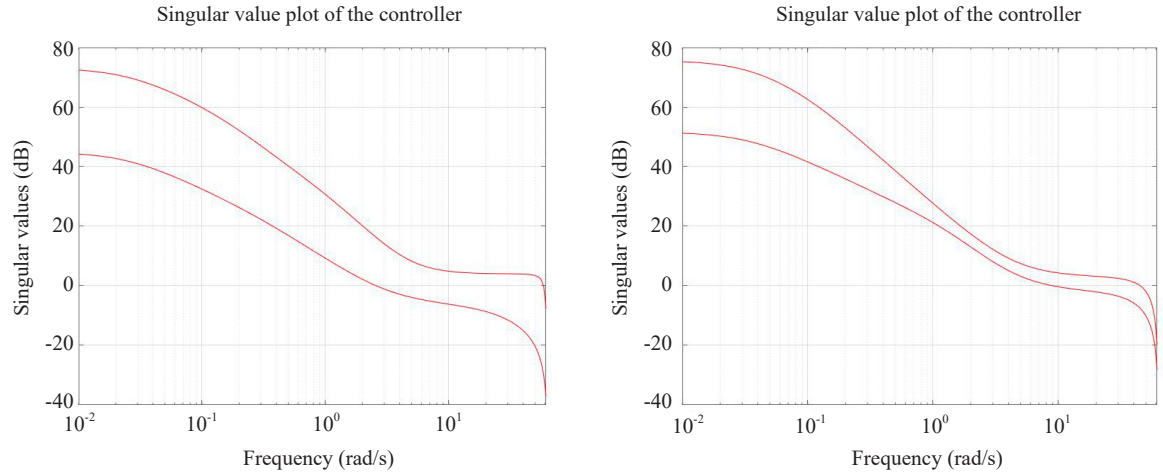

Figure 17. Controller singular value plots for the black-box (left) and gray-box (right) identification models

The controller singular values for both types of models are as shown in Figure 17. The controller based on the gray box model ensures closer gain of the two channels.

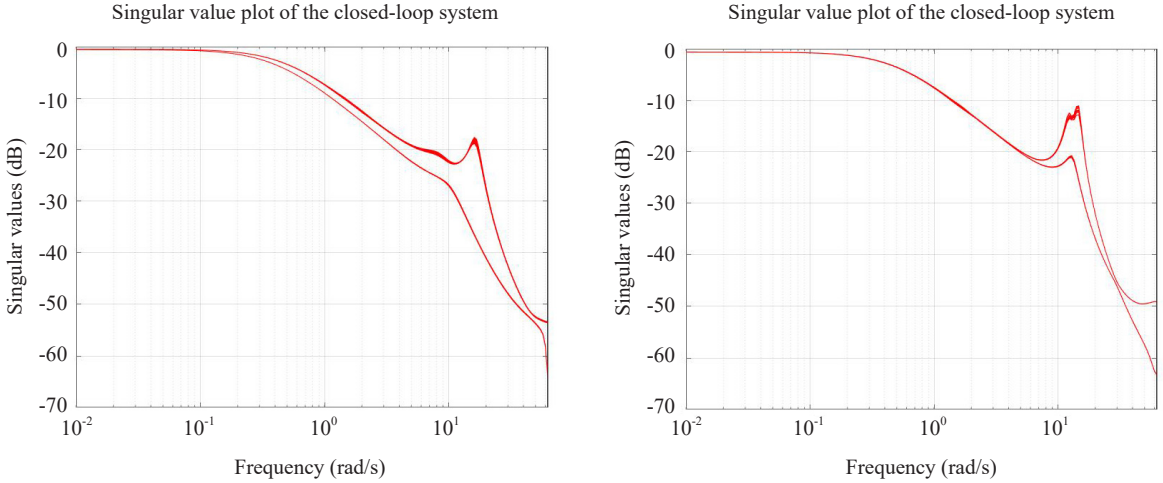

Figure 18. Closed-loop system singular value plots for the black-box (left) and gray-box (right) identification models

From the closed-loop singular value plots as shown in Figure 18, one can conclude that both systems have a closed-loop bandwidth of about 0.4 rad/s. Obviously, the two closed-loop systems have close behavior in the frequency domain.

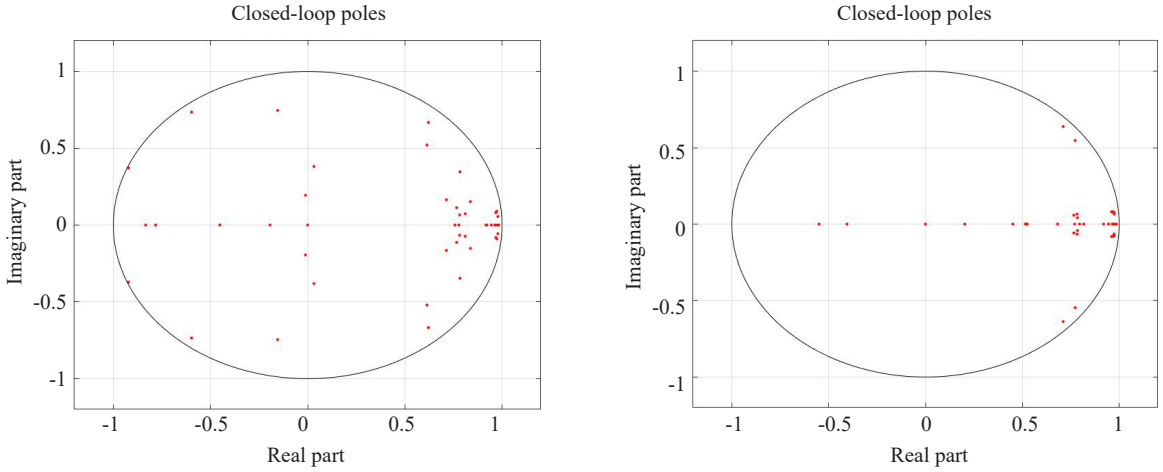

Figure 19. Closed-loop system poles for the black-box (left) and gray-box (right) identification models

The closed-loop poles for both systems are shown in Figure 19. Although the two systems have similar behavior, the closed-loop poles are distributed differently.

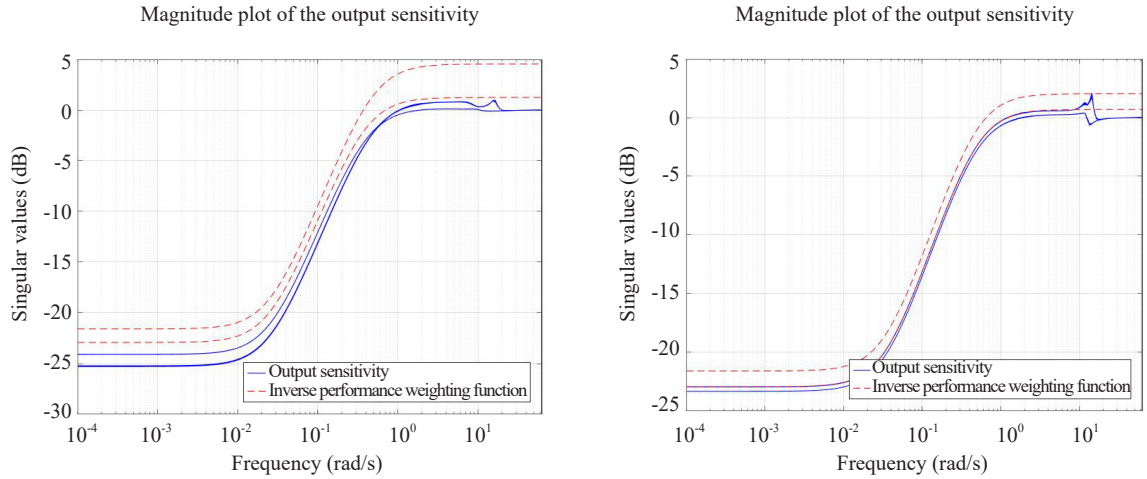

Figure 20. Closed-loop system output sensitivity for the black-box (left) and gray-box (right) identification models

The plots of output sensitivity functions, as shown in Figure 20 prove that both systems reject sufficiently well disturbances with the frequency band up to 10^{-2}-10^{-1} rad/s.

The plots of input sensitivity functions for both systems are compared in Figure 21. For both systems, there are peaks of the frequency responses near 10 rad/s, which shows increased sensitivity of the input actions to noises within such frequency.

The robust stability μ-plots obtained by the function robstab as shown in Figure 22 demonstrate that the two systems have close robustness properties. The maximum sensitivity to parameter variations is within the frequency interval of 1-2 rad/s.

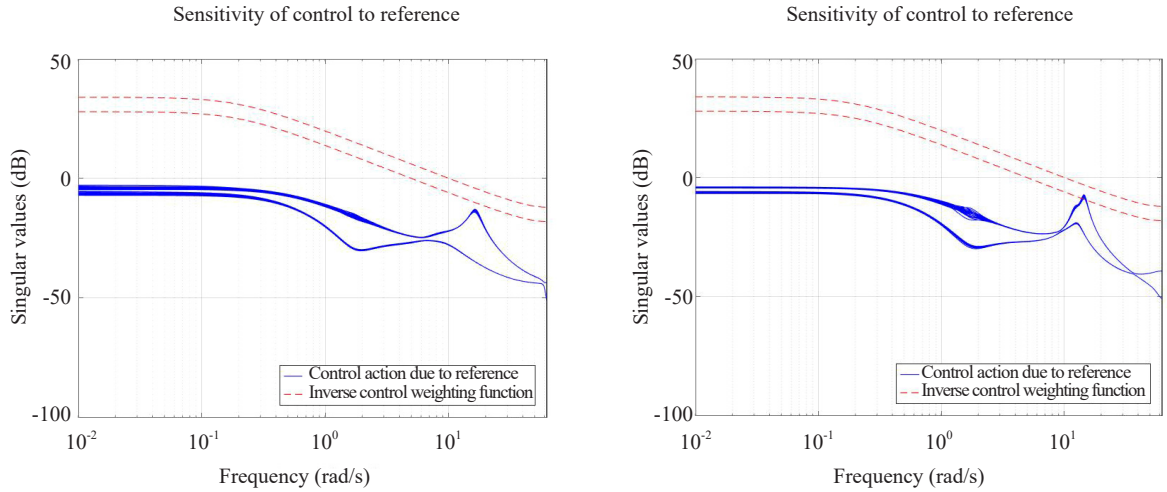

Figure 21. Closed-loop system input sensitivity for the black-box (left) and the gray-box (right) identification models

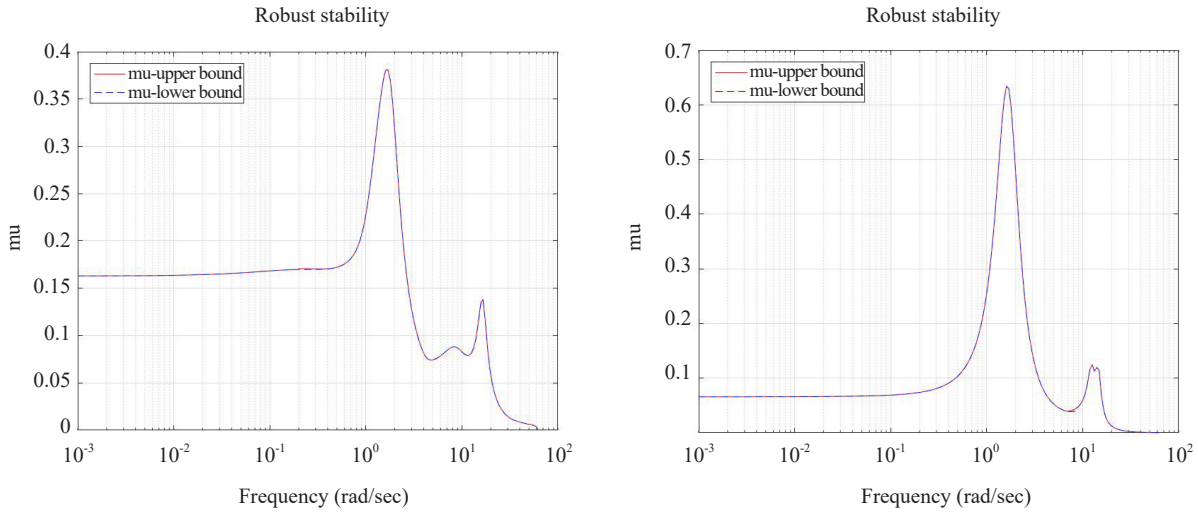

Figure 22. Robust stability of the closed-loop system for black-box (left) and gray-box (right) identification models

6. Embedding of the robust controller

After a suitable controller is determined, it is possible to go to the next design step, which is generating control code from the Simulink® controller model.

By using MATLAB® and Simulink®, the designer can automatically generate the control code, which increases efficiency, improve performance, and promote the innovation of control algorithms.

One of the widely used technologies for automatic generation of code intended for loading in microcontrollers and DSP is based on the programming tools Simulink Coder™ and Embedded Coder®, which are included in the programming system MATLAB®.

The Simulink Coder™ [21] (formerly known as Real-Time Workshop) generates and executes C and C++ code from Simulink® block-diagrams, diagrams of Stateflow® and MATLAB® functions. The generated output code can be used in applications in real-time and non-real-time, including accelerated simulation, rapid prototyping, and hardware-in-the-loop simulation. The generated code can be tuned and debugged using Simulink or can be executed out of MATLAB® and Simulink®.

Embedded Coder® [22] generates compact and fast C and C++ code for using embedded processors and

microcontrollers for mass production. Embedded Coder® gives additional opportunities for configuration MATLAB® Coder™ and Simulink Coder™ and optimization of the generated code, files, and data. These optimizations improve the coding efficiency and facilitate the integration with previous code, data types, and calibration parameters, used in the embedding. The Embedded Coder® supports software-in-the-loop (SIL) and processor-in-the loop (PIL) simulations.

In this case, the designed μ-controllers are of 16th order. They were implemented in an embedded control system to steer the real analog model. The controllers were embedded in the control board *Arduino Due* based on the *Atmel SAM3X8E ARM Cortex-M3* CPU [20] by code generation from Simulink model with help of Simulink Coder™. This board works at 84 MHz and may perform single-precision (32-bit) computations by using FPU (Floating-Point Unit). It possesses low-performance 10-bits A/D converters and 12-bits D/A converters. The block diagram of the designed embedded robust control system is presented in Figure 23.

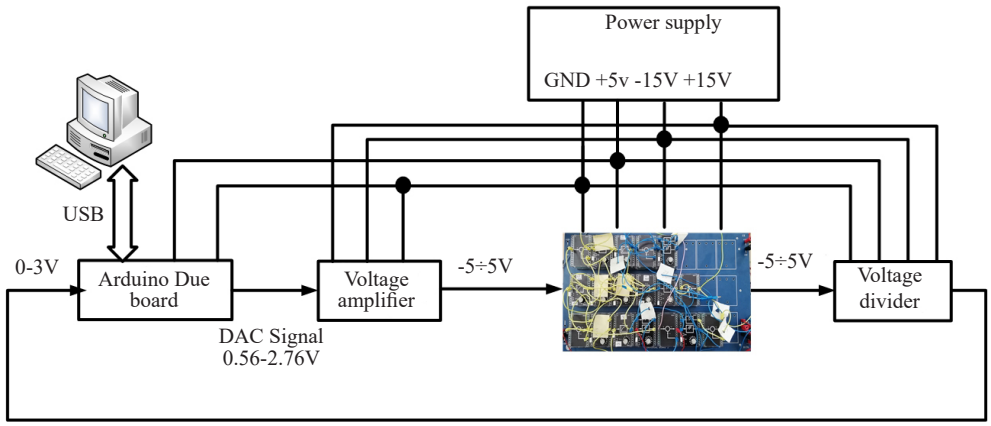

Figure 23. Block diagram of embedded robust control system

The developed specialized Simulink model used for control code generation is shown in Figure 24. The main block is a subsystem named *Single-Precision Controller*, which represents the state-space realization of designed μ-controllers.

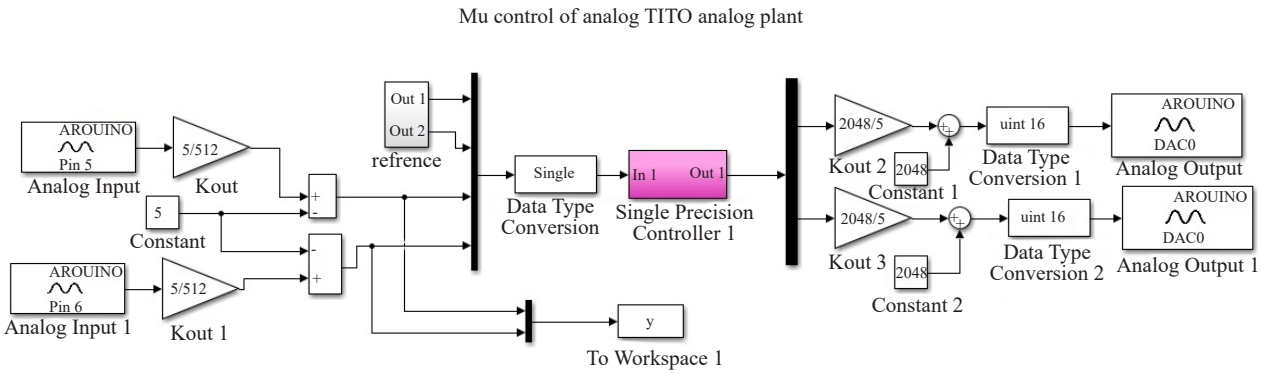

Figure 24. Simulink model for control code generation

The Simulink model also includes the blocks “Analog input” and “Analog Output” which were taken from the specialized library Simulink Support Package for Arduino Hardware. These blocks were used to interface with the ADC and Digital to Analog Converter (DAC) converters of Arduino board.

7. Experimental results

Several experiments with developed embedded control systems were done. A comparison between results from the experiment and Matlab simulation was performed. The output signals from experiments and simulation for the black box and gray box identification models are as shown in Figure 25 and 26 (all signals are measured in volts). In both cases, the μ-controller was implemented in single-precision (32 bits). The coincidence between experimental and simulation results is acceptable. The real outputs contained small noise due to random disturbances and noises in ADCs and DACs. The control actions contained larger noise in comparison with the outputs, as expected from the input sensitivity frequency response.

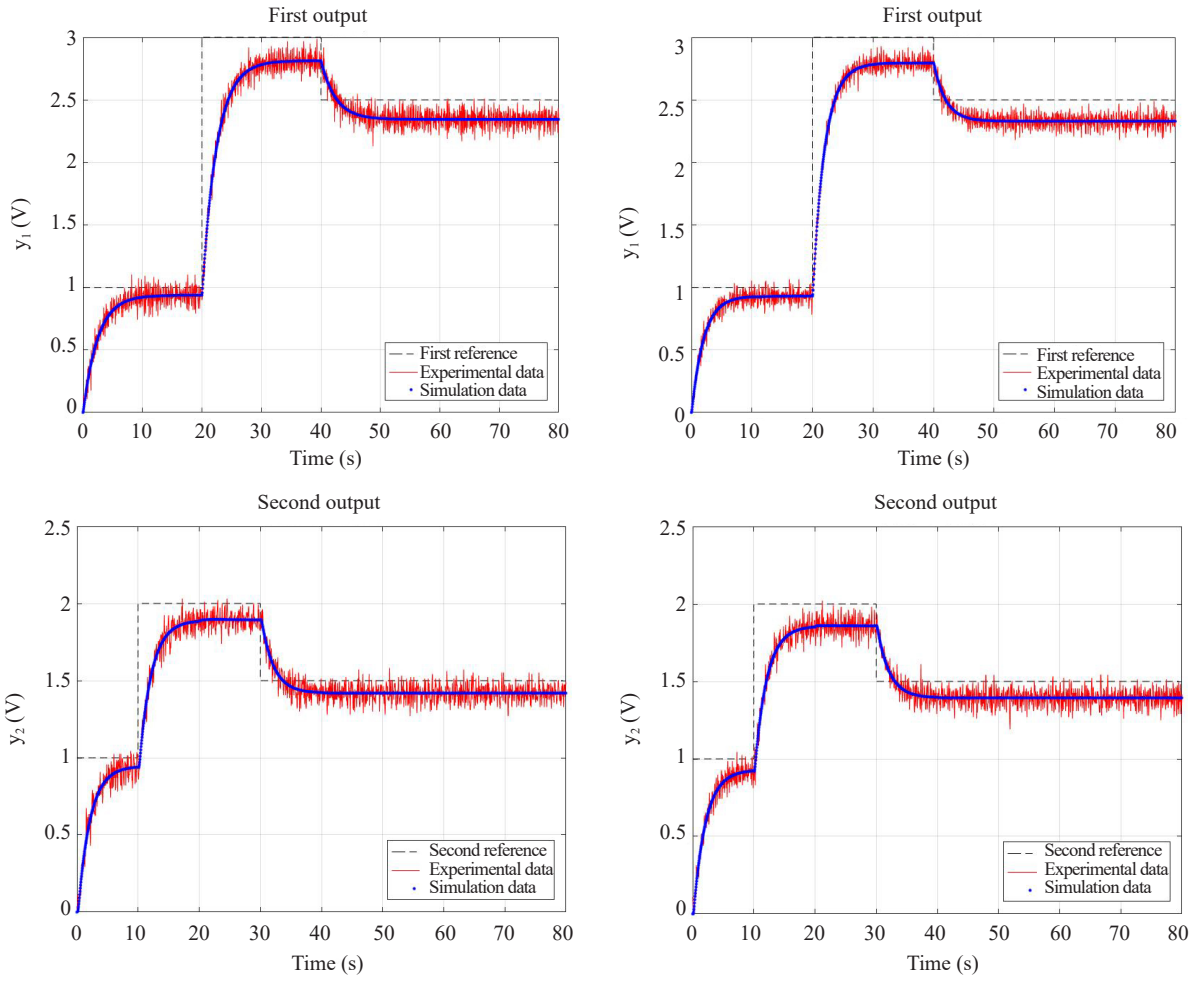

Figure 25. Actual and simulated output signals for the black-box (left) and the gray-box (right) identification models

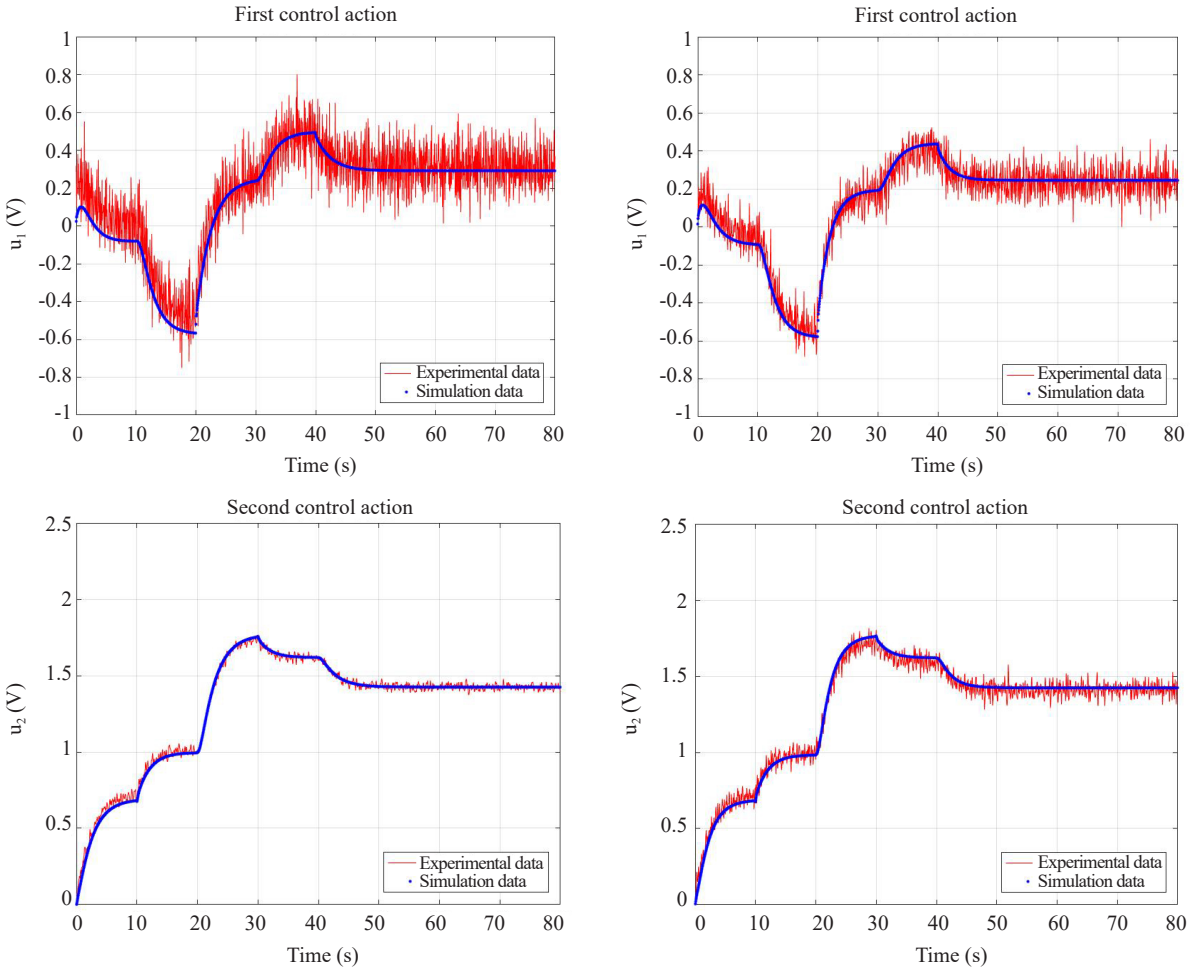

Figure 26. Actual and simulated control signals for the black-box (left) and the gray-box (right) identification models

8. Conclusions

The usage of black box or gray box identification to obtain unstructured uncertainty models intended for the design of robust controllers produced close and successful results. As one may expect, the derivation of the gray box uncertain model requires the implementation of weighting transfer functions of lower order. However, by using appropriate model reduction, the plant model order decreased sufficiently without sacrificing the closed-loop system behavior. A difficult question remains to obtain tighter bounds on the model uncertainty to reduce the conservatism in the controller design.

Acknowledgments

The authors would like to thank the Research and Development Sector at the Technical University of Sofia for financial support.

Conflict of interest

The authors declare no conflict of interest.

References

[1] P. Petkov, T. Slavov, and J. Kralev, "Embedded robust control of multivariable plants," In 19th IFAC Conference on Technology, Culture and International Stability TECIS' 2019, Sozopol, Bulgaria, 26-28 September 2019, *IFAC Papers Online*, vol. 52, no. 25, pp. 4-9, 2019. Available: DOI: 10.1016/j.ifacol.2019.12.436

[2] T. Slavov, J. Kralev, and P. Petkov, "Uncertain modeling and robust control of multivariable plants," *Comptes rendus de l'Académy Bulgare des Sciences*, vol. 72, no. 8, pp. 1095-1101, 2019.

[3] P. H. Petkov, T. N. Slavov, and J. K. Kralev. *Design of Embedded Robust Control Systems using MATLAB®/ Simulink®*. IET Control, Robotics, and Sensor Series 113. London: The Institution of Engineering and Technology, 2018.

[4] L. Ljung, *System Identification: Theory for the User*, 2nd ed., Englewood Cliffs, NJ: Prentice-Hall, Inc., 1999.

[5] L. Ljung, *System Identification Toolbox™ User's Guide*. Natick, MA: The Math Works Inc., 2016. Available: http://www.mathworks.com/help/pdf_doc/ident/ident_ug.pdf [Accessed 4th March 2021].

[6] M. Gevers, "Identification for control: From the early achievements to the revival of experiment design," *European Journal of Control*, vol. 11, pp. 335-352, 2005. Available: DOI: 10.3166/ejc.11.335-352

[7] H. Hjalmarsson, "From experiment design to closed-loop control," *Automatica*, vol. 41, pp. 393-438, 2005. Available: DOI: 10.1016/j.automatica.2004.11.021

[8] M. L. Darby and M. Nikolaou, "Identification test design for multivariable model-based control: An industrial perspective," *Control Engineering Practice*, vol. 22, pp. 165-180, 2014. Available: DOI: 10.1016/j.conengprac.2013.06.018

[9] *Serie 9500 Modulsystem Regelungstechnik*. hps-SystemTechnik, 2019. Available: http://hps-systemtechnik.com/hps-board-line-2/control-engineering [Accessed 4th March 2021].

[10] J. L. Figueroa and S. I. Biagiola, "Modelling and uncertainties characterization for robust control," *Journal of Process Control*, vol. 23, pp. 415-428, 2013. Available: DOI: 10.1016/j.jprocont.2012.11.008

[11] S. Gugercin, A. Antoulas, and H. P. Zhang, "An approach to identification for robust control," *IEEE Transactions on Automatic Control*, vol. 48, pp. 1109-1115, 2003. Available: DOI: 10.1109/TAC.2003.812821

[12] S. G. Douma and P. M. J. Van den Hof, "Relations between uncertainty structures in identification for robust control," *Automatica*, vol. 41, pp. 439-457, 2005. Available: DOI: 10.1016/j.automatica.2004.11.005

[13] P. Van den Hof, "Identification of experimental models for control design," Proceedings of the 18th Instrumentation and Measurement Technology Conference (IMTC 2001), 21-23 May 2001, Budapest, Hungary. IEEE, 2001, pp. 1155-1162. Available: DOI 10.1109/IMTC.2001.928260

[14] R. S. Smith and J. C. Doyle, "Model validation: A connection between robust control and identification," *IEEE Transactions on Automatic Control*, vol. 37, pp. 942-952, 1992. Available: DOI:10.1109/9.148346

[15] S. Venkatesh, "Identification of uncertain systems described by Linear Fractional Transformations," In proceedings of the 42nd IEEE Conference and Decision and Control, Maui, Hawaii, USA, December, 2003, pp. 5532-5537. Available: DOI 10.1109/CDC.2003.1272518

[16] K. Zhou, J. C. Doyle, and K. Glover, *Robust and Optimal Control*. Upper Saddle River, NJ: Prentice-Hall, 1996.

[17] S. Skogestad and I. Postlethwaite, *Multivariable Feedback Control. Analysis and Design*, 2nd ed., Chichester, England: John Wiley & Sons, 2005.

[18] D. W. Gu, P. H. Petkov, and M. M. Konstantinov, *Robust Control Design with MATLAB®*, 2nd ed., London: Springer, 2013. Available: DOI 10.1007/978-1-4471-4682-7

[19] G. Balas, R. Chiang, A. Packard, and M. Safonov, *Robust Control Toolbox User's Guide*. Natick, MA: The Math Works, Inc., 2020. Available: http://www.mathworks.com/help/pdf_doc/robust/robust_ug.pdf [Accessed 4th March 2021].

[20] *Arduino Due Technical Specifications*. Arduino. 2021. Available: https://store.arduino.cc/arduino-due [Accessed 4th March 2021].

[21] *Simulink® Coder™ User's Guide*, Natick, MA: The MathWorks, Inc., 2020. Available: http://www.mathworks.com/help/pdf_doc/rtw/rtw_ug.pdf [Accessed 4th March 2021].

[22] *Embedded Coder® User's Guide*, Natick, MA: The MathWorks, Inc., 2020. Available: http://www.mathworks.com/help/pdf_doc/ecoder/ecoder_ug.pdf [Accessed 4th March 2021].